Charm Production Near Threshold

R. Vogt

Nuclear Science Division, Lawrence Berkeley National Laboratory, Berkeley, CA 94720, USA
Physics Department, University of California, Davis, CA 95616, USA

Preliminary Remarks

I'm going to talk about near threshold hadroproduction of heavy quarks

Near threshold because full NNLO calculation is not yet available, don't even know if anyone's working on it

Discussion relevant for GSI facility with $p_{\text{beam}} = 25$ GeV where $c\bar{c}$
production *is* near threshold

Describe our calculation up to NNLL (N. Kidonakis, E. Laenen, S. Moch, and R. V., Phys. Rev. **D64** (2001) 114001; Nucl. Phys. **A715** (2003) 549c; Phys. Rev. **D67** (2003) 211) and results beyond NNLL (N. Kidonakis and R.V., Phys. Rev. **D68** (2003) 114014 and hep-ph/0401056.

Introduction to NNLO

pQCD works best when coupling is small and expansion converges in the first 1-2 terms

Factorized hadroproduction cross section

$$\sigma_{h_1 h_2 \to Q\overline{Q}X}(S, m^2) = \sum_{i,j=q,\overline{q},g} \int dx_1 dx_2 \, f_{i/h_1}(x_1, \mu^2) \, f_{j/h_2}(x_2, \mu^2) \times \sigma_{ij \to Q\overline{Q}X'}(x_1, x_2, \mu^2)$$

Parton densities, $f_{i/h}$, are universal and nonperturbative

σ is hard-scattering kernel calculable in pQCD

Imperfect separation of scales near partonic threshold, $s \sim 4m^2$

Comparison of pQCD to total cross section data shows important differences

NLO correction as big as LO cross section for 'light' heavy quarks

$$\sigma = \sigma_{\rm Born}\left(1 + a_1 \frac{\alpha_s}{\pi} + a_2 \frac{\alpha_s^2}{\pi^2} + \cdots\right)$$

When will the series converge?

Resummed Cross Section

Leading Log (LL): universal, based on comparison to Drell-Yan (Laenen, Smith and van Neerven)

Cross section grows like $\exp(E)$ where

$$E \sim \int_0^\infty \frac{d\omega}{\omega}(1-\exp(-N\omega))\{\frac{\nu(\alpha_s(f(\omega)))}{2} + \int_{\omega^2}^1 \frac{d\lambda}{\lambda} A(\alpha_s(f(\sqrt{\lambda})))\}$$

Next-to-Leading Log (NLL): color flow, process specific (Kidonakis and Sterman, Kidonakis, Smith and R.V.)

Exponents grow large because α_s blows up in integration

Prescription required to bring cross section under control

Finite Order Expansion

Resummed cross section is used as generator of NNLO cross section

Results first available to NNLL *in the expansion* (Kidonakis, Laenen, Moch and R.V.)

$b\overline{b}$ and $c\overline{c}$ results now available beyond NNLL (Kidonakis and R.V.)

Now

$$\exp(E) \sim 1 + \frac{\alpha_s(\mu)}{\pi} \sum_{k=0}^{2} C_k^{(1)} \ln^k N + \frac{\alpha_s^2(\mu)}{\pi^2} \sum_{k=0}^{4} C_k^{(2)} \ln^k N + \cdots$$

No cutoff or other prescription needed

Based on $q\overline{q}$ and gg channels

Complication — final result depends on distance from partonic threshold which depends on how the integration is done, either by integrating away momentum of one quark (one particle inclusive – 1PI) or if the $Q\overline{Q}$ is treated as a pair (pair invariant mass – PIM)

Partonic cross section calculated by defining scale independent coefficient functions multiplying powers of $\ln(\mu^2/m^2)$ in each kinematics

gg channel most dependent on kinematics choice, dominant for $b\overline{b}$ and $c\overline{c}$ production

One-Particle Inclusive (1PI) Kinematics

Momentum of unobserved Q ($\overline{Q}$) integrated away

$$p(P_1)+p(P_2)\longrightarrow Q(p_1)+X(p_X)\,,$$

X contains heavy antiquark and any additional partons

Interaction on partonic level at LO

$$\begin{aligned} q(k_1)+\overline{q}(k_2) &\longrightarrow Q(p_1)+X[\overline{Q}](p_2') \\ g(k_1)+g(k_2) &\longrightarrow Q(p_1)+X[\overline{Q}](p_2') \end{aligned}$$

At LO or $X[\overline{Q}](p_2')\equiv\overline{Q}(\overline{p}_2)$, at partonic threshold with $\overline{Q}$ momentum $\overline{p}_2$

Heavy quarks aren't produced at rest but $p_1=-p_2'$

Partonic Mandelstam invariants:

$$\begin{aligned} s=(k_1+k_2)^2 \quad &, \quad t_1=(k_2-p_1)^2-m^2\,, \\ u_1=(k_1-p_1)^2-m^2 \quad &, \quad s_4=s+t_1+u_1 \end{aligned}$$

s_4 is inelasticity of partonic reaction: $s_4=(p_2')^2-m^2$, $p_2'=\overline{p}_2+k$, $s_4=0$ at threshold

When k is small, define distance from partonic threshold as weight

$$\omega_{1\mathrm{PI}}=\frac{s_4}{m^2}\simeq\frac{2\overline{p}_2\cdot k}{m^2}\equiv\frac{2\zeta_{1\mathrm{PI}}\cdot k}{m}$$

Singular functions in 1PI:

$$\left[\frac{\ln^l(s_4/m^2)}{s_4}\right]_+$$

Pair Invariant Mass (PIM) Kinematics

$Q\overline{Q}$ pair treated as a unit

$$p(P_1)+p(P_2)\longrightarrow Q\overline{Q}(p')+X(p_X)\,,$$

Partonic interactions at LO

$$\begin{aligned} q(k_1)+\overline{q}(k_2) &\longrightarrow Q\overline{Q}(p')+X'(k)\\ g(k_1)+g(k_2) &\longrightarrow Q\overline{Q}(p')+X'(k)\end{aligned}$$

Heavy quark pair mass squared is $p'^2=M^2$

Partonic threshold, $X'(k)=0$ and

Mandelstam invariants at partonic threshold:

$$s=M^2\,,\quad t_1=-\frac{M^2}{2}(1-\beta_M\cos\theta)\,,\quad u_1=-\frac{M^2}{2}(1+\beta_M\cos\theta)$$

$\beta_M=\sqrt{1-4m_Q^2/M^2}$ and θ is the scattering angle in the parton center of mass frame

PIM distance from threshold represented by weight

$$\omega_{\rm PIM}=1-z=1-\frac{M^2}{s}\simeq\frac{2p'\cdot k}{s}\equiv\frac{2\zeta_{\rm PIM}\cdot k}{\sqrt{s}}$$

Singular functions in PIM:

$$\left[\frac{\ln^l(1-z)}{1-z}\right]_+$$

Total Partonic Cross Sections

1PI total cross section

$$\sigma_{ij}(s,m^2,\mu^2) = \int d(-t_1) \int d(-u_1) \frac{d^2\sigma_{ij}(s,t_1,u_1)}{dt_1 du_1}$$

PIM total cross section

$$\sigma_{ij}(s,m^2,\mu^2) = \int d\cos\theta \int dM^2 \frac{d^2\sigma_{ij}(s,M^2,\cos\theta)}{dM^2 d\cos\theta}$$

The total partonic cross sections in both kinematics can be expressed in terms of dimensionless scaling functions $f_{ij}^{(k,l)}(\eta)$ where $\eta = s/4m^2 - 1$, $\eta \ll 1$ closest to partonic threshold

Thus

$$\begin{aligned}\sigma_{ij}(s,m^2,\mu^2) \;=\; & \frac{\alpha_s^2(\mu)}{m^2}\Bigg[f_{ij}^{(0,0)}(\eta) \\ & + 4\pi\alpha_s(\mu)\left(f_{ij}^{(1,0)}(\eta) + f_{ij}^{(1,1)} \ln\left(\frac{\mu^2}{m^2}\right)\right) \\ & + (4\pi\alpha_s(\mu))^2\left(f_{ij}^{(2,0)}(\eta) + f_{ij}^{(2,1)} \ln\left(\frac{\mu^2}{m^2}\right) + f_{ij}^{(2,2)} \ln^2\left(\frac{\mu^2}{m^2}\right)\right) \\ & + \sum_{k=3}^{\infty} (4\pi\alpha_s(\mu))^k \sum_{l=0}^{k} f_{ij}^{(k,l)}(\eta)\, \ln^l\left(\frac{\mu^2}{m^2}\right)\Bigg]\end{aligned}$$

We construct LL, NLL, NNLL and subleading approximations to scaling functions in $q\bar{q}$ and gg channels

Exact results for $f_{ij}^{(1,1)}$, $f_{ij}^{(2,1)}$, and $f_{ij}^{(2,2)}$ derived using renormalization group methods, $k = 1$ results can be checked against earlier calculations

Hierarchy of Logs (1PI)

$f_{ij}^{(1,0)}$, NLO:

- LL: $[\ln(s_4/m^2)/s_4]_+$
- NLL: $[1/s_4]_+$
- NNLL: $\delta(s_4)$

$f_{ij}^{(1,1)}$, NLO:

- LL: $[1/s_4]_+$
- NLL, NNLL: $\delta(s_4)$

$f_{ij}^{(2,0)}$, NNLO:

- LL: $[\ln^3(s_4/m^2)/s_4]_+$
- NLL: $[\ln^2(s_4/m^2)/s_4]_+$
- NNLL: $[\ln(s_4/m^2)/s_4]_+$
- NNNLL: $[1/s_4]_+$
- ζ terms: $\delta(s_4)$

$f_{ij}^{(2,1)}$, NNLO:

- LL: $[\ln^2(s_4/m^2)/s_4]_+$
- NLL: $[\ln^1(s_4/m^2)/s_4]_+$
- NNLL: $[1/s_4]_+$
- NNNLL: $\delta(s_4)$

$f_{ij}^{(2,2)}$, NNLO:

- LL: $[\ln(s_4/m^2)/s_4]_+$
- NLL: $[1/s_4]_+$
- NNLL: $\delta(s_4)$

The $q\bar{q}$ One-Loop Scaling Functions in 1PI and PIM

PIM agrees somewhat better with exact results

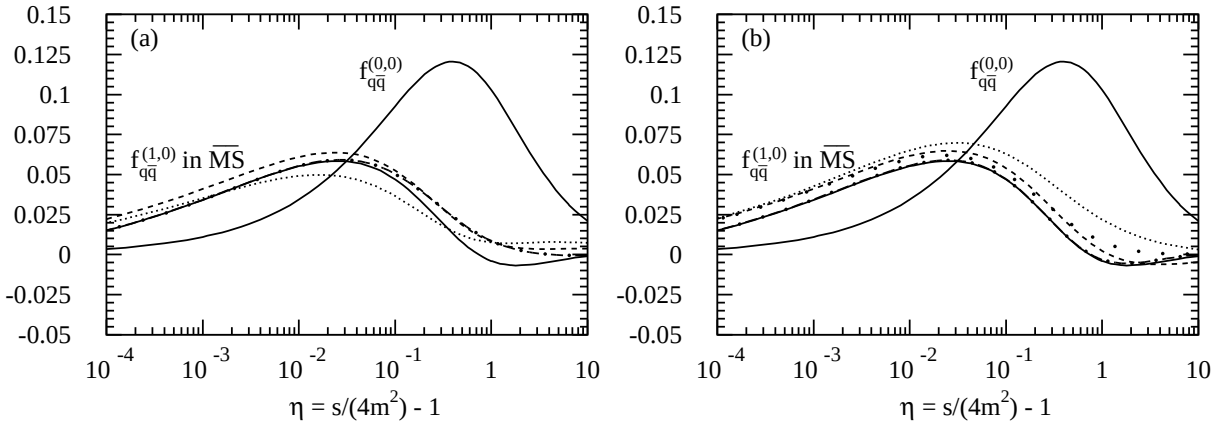

Figure 1: (a) The functions $f_{q\bar{q}}^{(k,0)}$, $k = 0, 1$ in the $\overline{\text{MS}}$-scheme and 1PI. We show the exact results for $f_{q\bar{q}}^{(k,0)}$, $k = 0, 1$ (solid), and, for $f_{q\bar{q}}^{(1,0)}$, the LL (dotted), the NLL (dashed) and the NNLL (dot-dashed) approximations. (b) The same in PIM. The spaced-dotted curve is an approximation involving the leading two powers of $\ln\beta$.

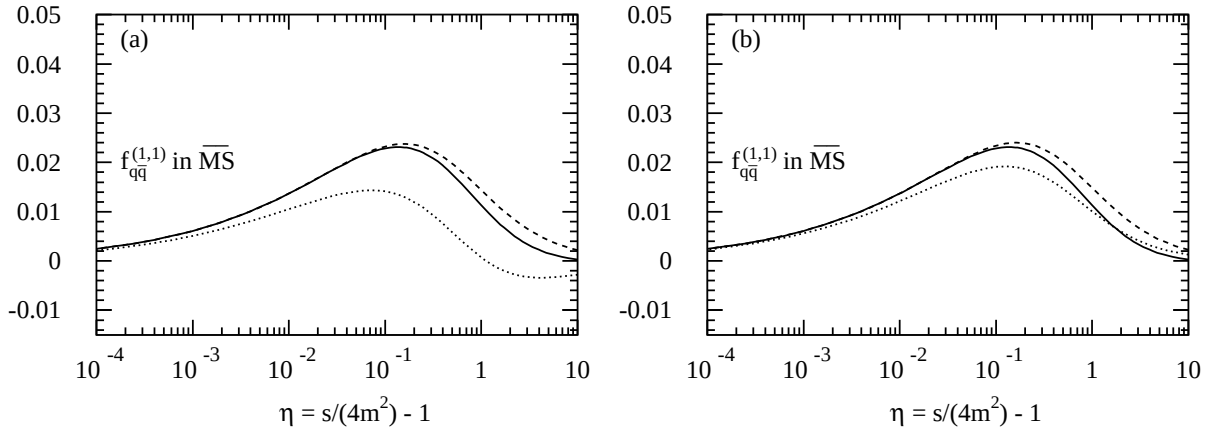

Figure 2: (a) The functions $f_{q\bar{q}}^{(1,1)}$ in 1PI. We show the exact result (solid) as well as the LL (dotted) and the NLL (dashed) approximations. There is no NNLL result for $f_{q\bar{q}}^{(1,1)}$. (b) The same in PIM.

The $q\bar{q}$ Two-Loop Scaling Functions in 1PI and PIM

PIM agreement better with exact results for $f_{q\bar{q}}^{(2,1)}$ and $f_{q\bar{q}}^{(2,2)}$

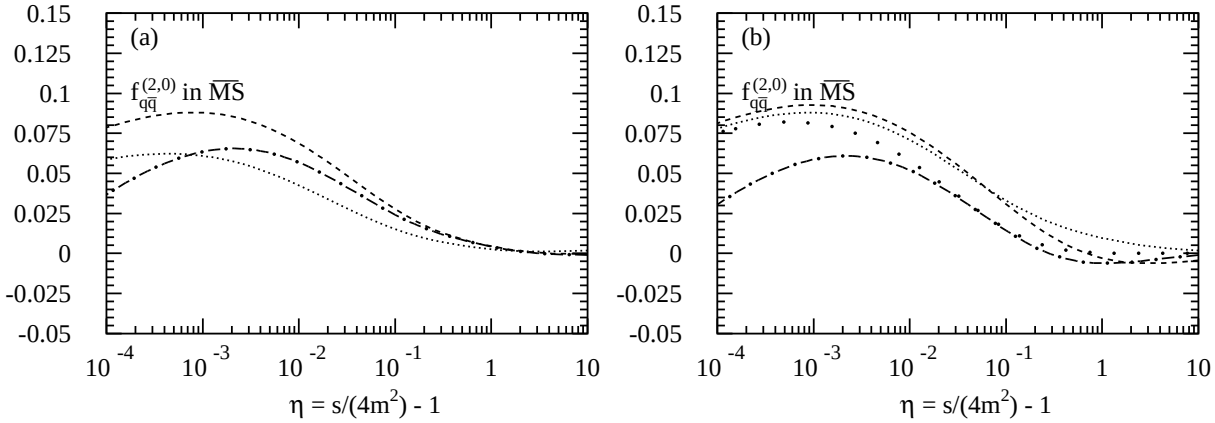

Figure 3: (a) The functions $f_{q\bar{q}}^{(2,0)}$ in the $\overline{\rm MS}$-scheme and 1PI. We show the LL (dotted), the NLL (dashed) and the NNLL (dot-dashed) approximations. (b) The same in PIM. The spaced-dotted curve is an approximation involving the leading two powers of $\ln\beta$. There are no exact results for $f_{q\bar{q}}^{(2,0)}$.

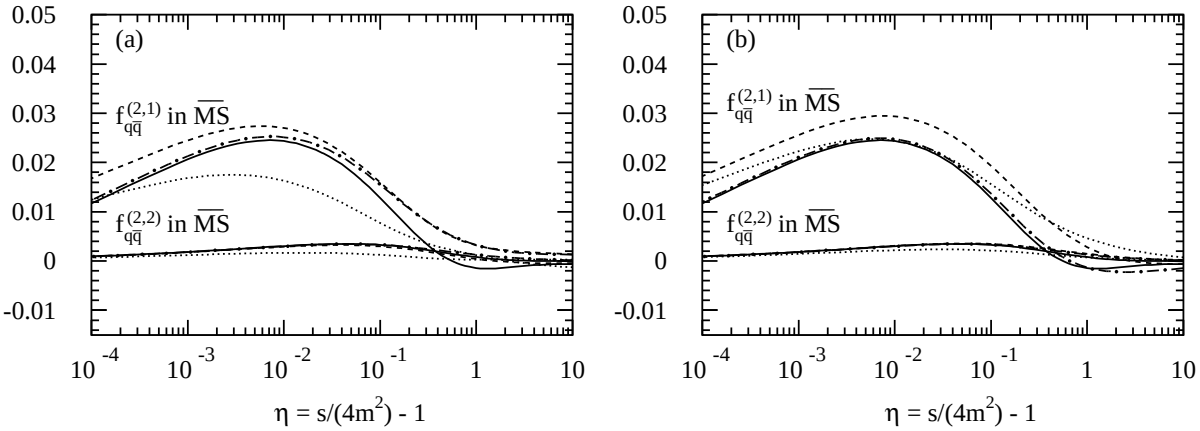

Figure 4: (a) The functions $f_{q\bar{q}}^{(2,1)}$ ($\overline{\rm MS}$) and $f_{q\bar{q}}^{(2,2)}$ in 1PI. We show the exact result (solid) and the LL (dotted), the NLL (dashed), and the NNLL (dot-dashed) approximations. (b) The same in PIM.

The *gg* One-Loop Scaling Functions in 1PI and PIM

1PI agrees somewhat better with exact result

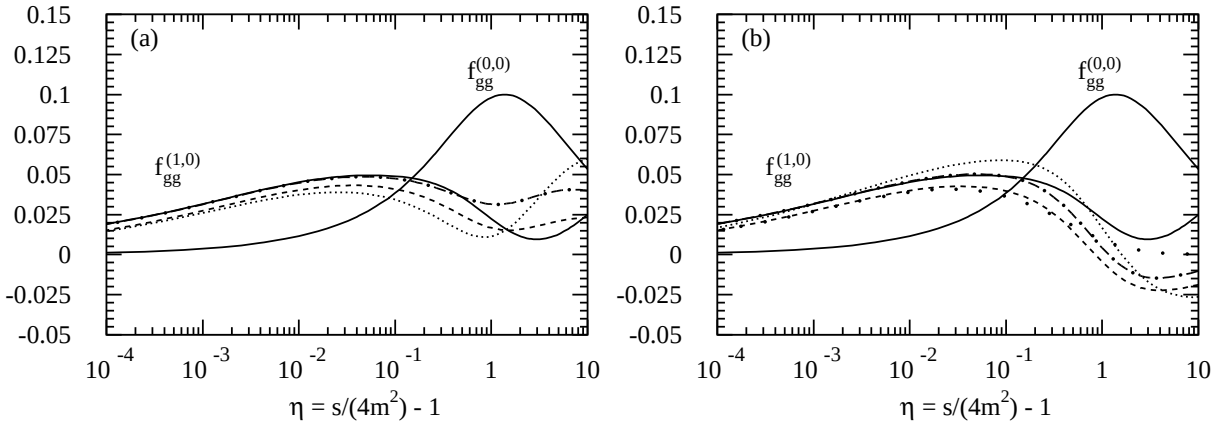

Figure 5: (a) The functions $f_{gg}^{(k,0)}$, $k = 0, 1$ in 1PI. We show the exact results for $f_{gg}^{(k,0)}$, $k = 0, 1$ (solid), and, for $f_{gg}^{(1,0)}$, the LL (dotted), the NLL (dashed) and the NNLL (dot-dashed) approximations. (b) The same in PIM. The spaced-dotted curve is an approximation involving the leading two powers of $\ln\beta$.

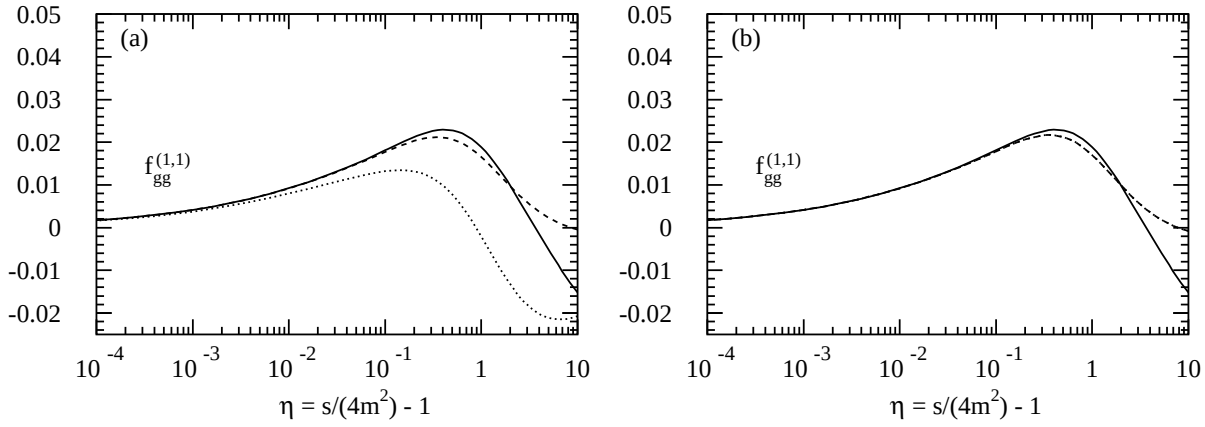

Figure 6: (a) The function $f_{gg}^{(1,1)}$ in 1PI. We show the exact result (solid) as well as the LL (dotted) and the NLL (dashed) approximations. There is no NNLL result for $f_{gg}^{(1,1)}$. (b) The same in PIM.

The gg Two-Loop Scaling Functions in 1PI and PIM

1PI agrees somewhat better with exact results for $f_{gg}^{(2,1)}$ and $f_{gg}^{(2,2)}$, biggest difference between 1PI and PIM at large η

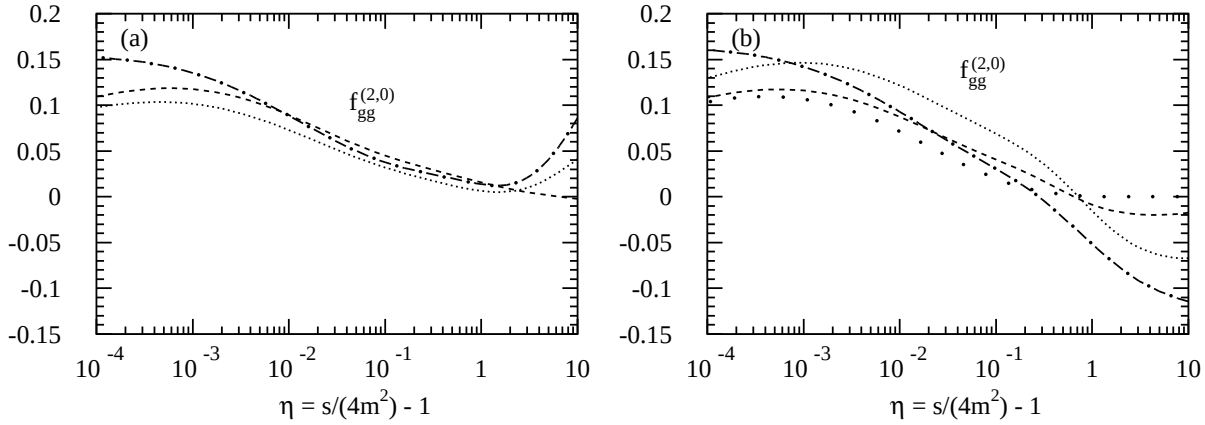

Figure 7: (a) The functions $f_{gg}^{(2,0)}$ in 1PI. We show the LL (dotted), the NLL (dashed) and the NNLL (dot-dashed) approximations. (b) The same in PIM. The spaced-dotted curve is an approximation involving the leading two powers of $\ln\beta$. There are no exact results for $f_{gg}^{(2,0)}$.

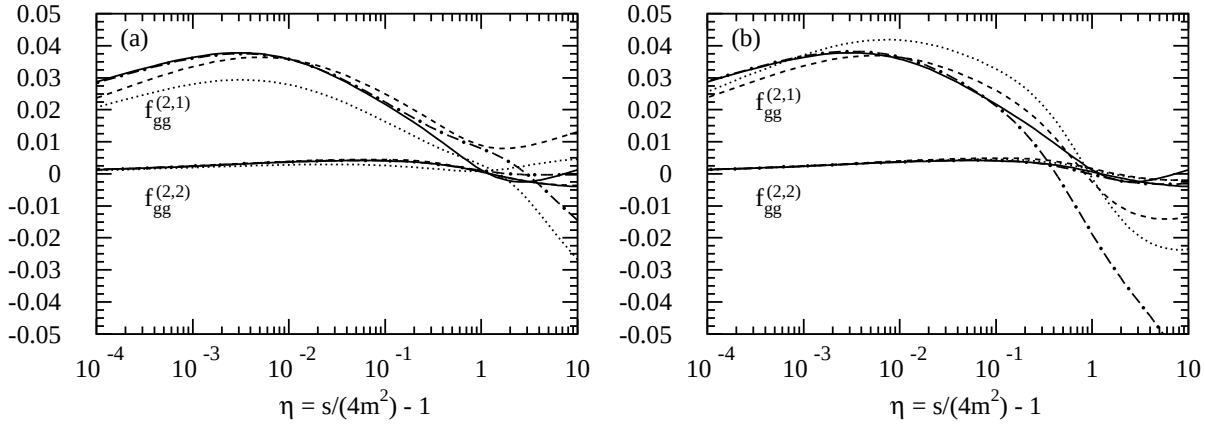

Figure 8: (a) The functions $f_{gg}^{(2,1)}$ and $f_{gg}^{(2,2)}$ in 1PI. We show the exact result (solid) as well as the LL (dotted), the NLL (dashed), and the NNLL (dot-dashed) approximations. (b) The same in PIM.

Parton Luminosity and Hadronic Cross Section

Typical hadron-hadron center of mass energies far from partonic threshold, $S \gg 4m^2$

However, validity of threshold approximation holds if parton densities give biggest contribution for $\eta < 1$

Parton luminosity is convolution of parton densities from the initial protons

$$\Phi_{ij}(\tau,\mu^2) = \tau \int_0^1 dx_1 \int_0^1 dx_2\, \delta(x_1 x_2 - \tau)\, \phi_{i/h_1}(x_1,\mu^2)\, \phi_{j/h_2}(x_2,\mu^2)$$

$\phi_{i/h}(x,\mu^2)$ is density of partons with flavor i in hadron h

Hadronic total cross section obtained by convoluting the parton flux with the partonic cross section

$$\begin{aligned}\sigma_{h_1 h_2}(S,m^2) &= \sum_{i,j=q,\overline{q},g} \int_{4m^2/S}^1 \frac{d\tau}{\tau}\, \Phi_{ij}(\tau,\mu^2)\, \sigma_{ij}(\tau S, m^2, \mu^2) \\ &= \sum_{i,j=q,\overline{q},g} \int_{-\infty}^{\log_{10}(S/4m^2-1)} d\log_{10}\eta\, \frac{\eta}{1+\eta} \ln(10)\, \Phi_{ij}(\eta,\mu^2)\, \sigma_{ij}(\eta, m^2, \mu^2)\end{aligned}$$

The second equality makes it easier to understand how close to threshold the reactions are

NNLL Approximation to NLO Cross Section Good

Comparing the exact NLO to NNLL approximation to NLO shows that the approximation is very good, particularly for the 1PI kinematics

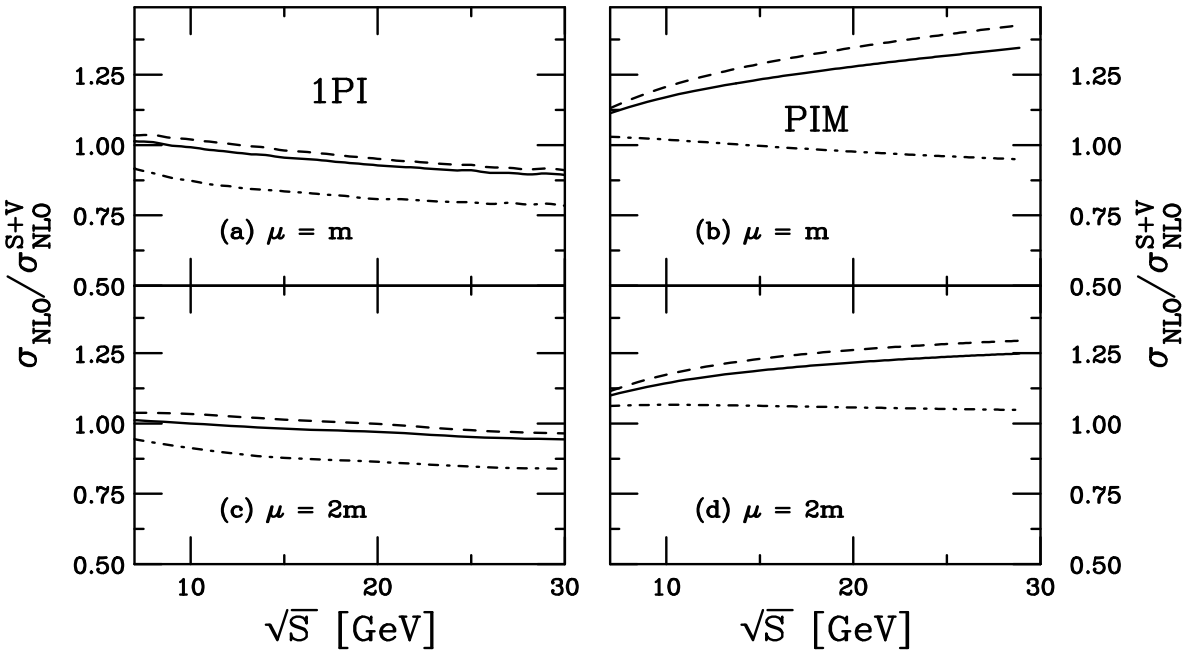

Figure 9: The ratios of the NLO exact, σ_{NLO} over the NLO soft-plus-virtual, σ_{NLO}^{S+V}, cross sections for charm quark production with $m = 1.5$ GeV are shown for the gg (dashed) and $q\bar{q}$ (dot-dashed) channels separately, along with their sum (solid).

Parton Luminosity at GSI

Both $q\bar{q}$ and gg luminosities weighted by factor $\ln(10)\eta/(1+\eta)$

Luminosities small in both channels but gg luminosity is larger, dominating total cross section

Peak of luminosities at $\eta \sim 0.15 - 0.3$, upper number for lower mass, no contributions from large η

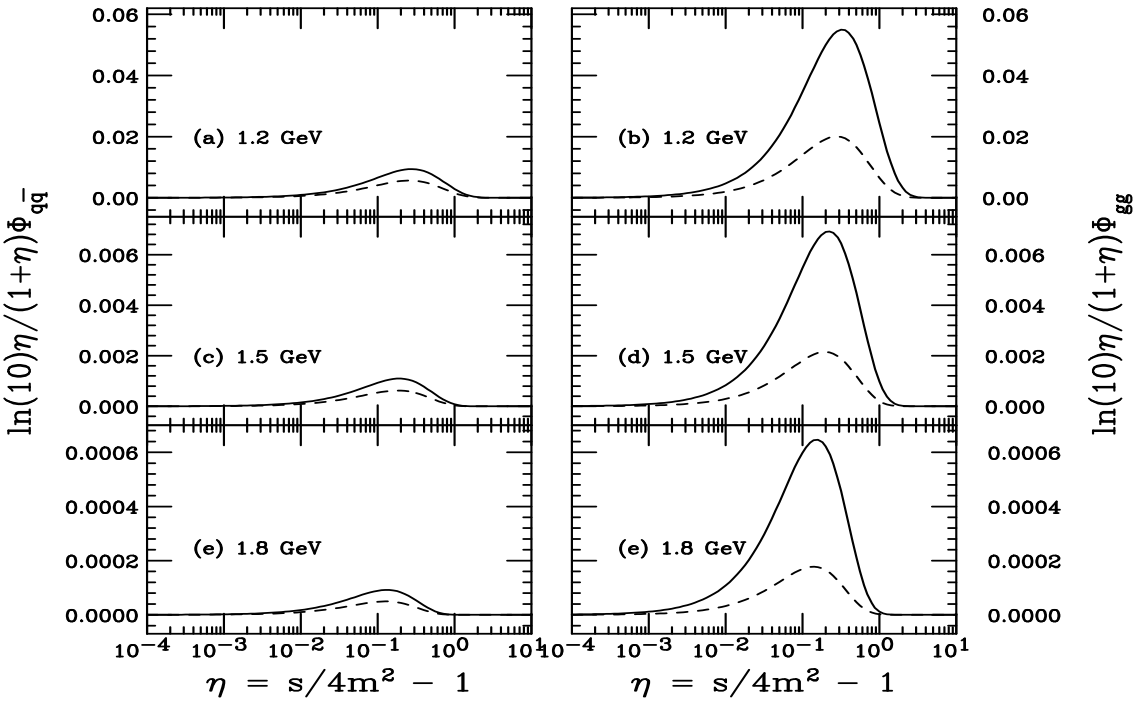

Figure 10: The parton luminosity at $\sqrt{S} = 6.98$ GeV with $m = 1.2$ GeV (upper), 1.5 GeV (middle) and 1.8 GeV (bottom) in the $q\bar{q}$ (left) and gg (right) channels. The solid curve is the result with $\mu = m$ while the dashed curves refer to $\mu = 2m$.

Charm quarks at threshold

Charm quark mass not well known, comparisons to data favor relatively low masses, we check range $1.2 \leq m \leq 1.8$ GeV with $\mu = m$ and $2m$

Results sensitive to choice of parton densities through value of $\Lambda^{(3)}_{\rm QCD}$ of global fit, the smaller the ratio $(\mu/\Lambda^{(3)}_{\rm QCD})^2$ in α_s, the larger the NNLO contribution

Beyond NNLL

We can go beyond NNLL to include subleading logarithms in the scaling functions

A master equation for simple and complex color flow can be derived to NNLO from the expanded resummed cross section, including logs subleading in the expanded cross section (N. Kidonakis)

The subleading logs are $\delta(s_4)$ ($\delta(1-z)$) in $f_{ij}^{(2,1)}$ (NNNLL) and $[1/s_4]_+$ (NNNLL), $\delta(s_4)$ (NNNNLL) ($[1/(1-z)]_+$, $\delta(1-z)$) in $f_{ij}^{(2,0)}$ in 1PI (PIM) kinematics

The full $\delta(s_4)$ contribution is not fully known, keep only terms from inversion of the Mellin transform at this level

Subleading Contributions to $f_{ij}^{(2,1)}$ in the $\overline{\rm MS}$ Scheme

Differences between 1PI and PIM kinematics already small at NNLL

Full $\delta(s_4)$ ($\delta(1-z)$) corrections to $f_{ij}^{(2,1)}$ are known, no need to second guess contribution from new terms

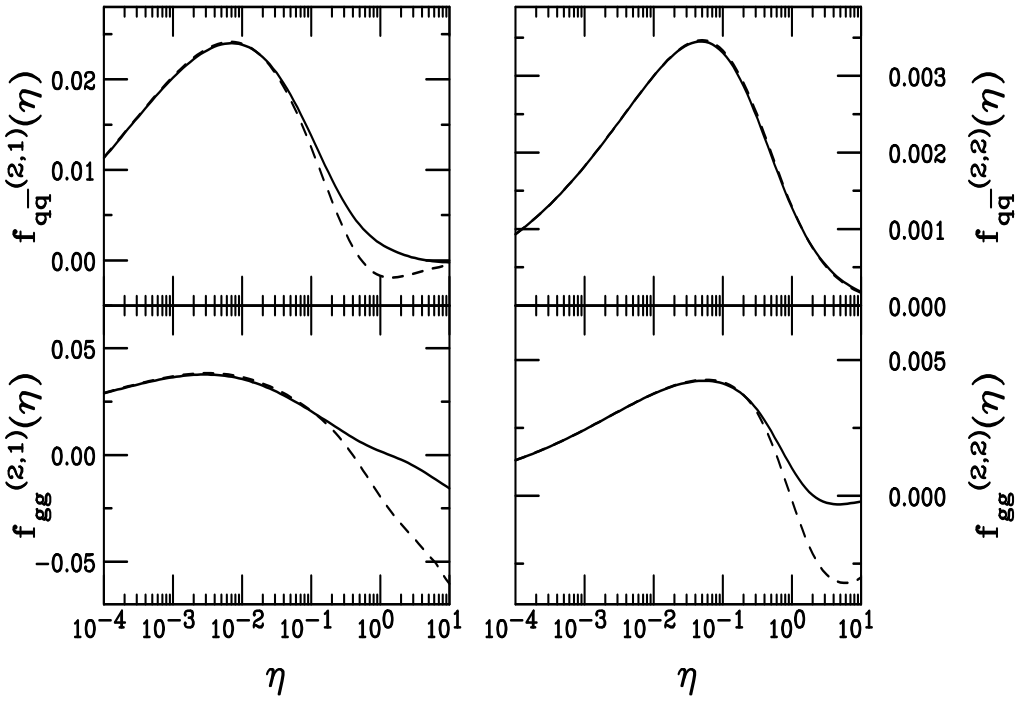

Figure 11: The $\overline{\rm MS}$ scheme scaling functions multiplying the scale-dependent logarithms, $f_{ij}^{(2,1)}$ (left-hand side) and $f_{ij}^{(2,2)}$ (right-hand side). The upper plots are for the $q\bar{q}$ channel while the lower plots are for the gg channel. The solid curves are for 1PI kinematics, the dashed for PIM kinematics. [From Kidonakis and R.V., Phys. Rev. **D 68** (2003) 114014.]

Subleading Contributions to $f_{ij}^{(2,0)}$ in the $\overline{\rm MS}$ Scheme

Differences between 1PI and PIM largely disappeared when $[1/s_4]_+$ ($[1/(1-z)]_+$) included

Beyond NNNLL we keep only 'ζ' terms from inversion from moment to momentum space in $\delta(s_4)$ ($\delta(1-z)$)

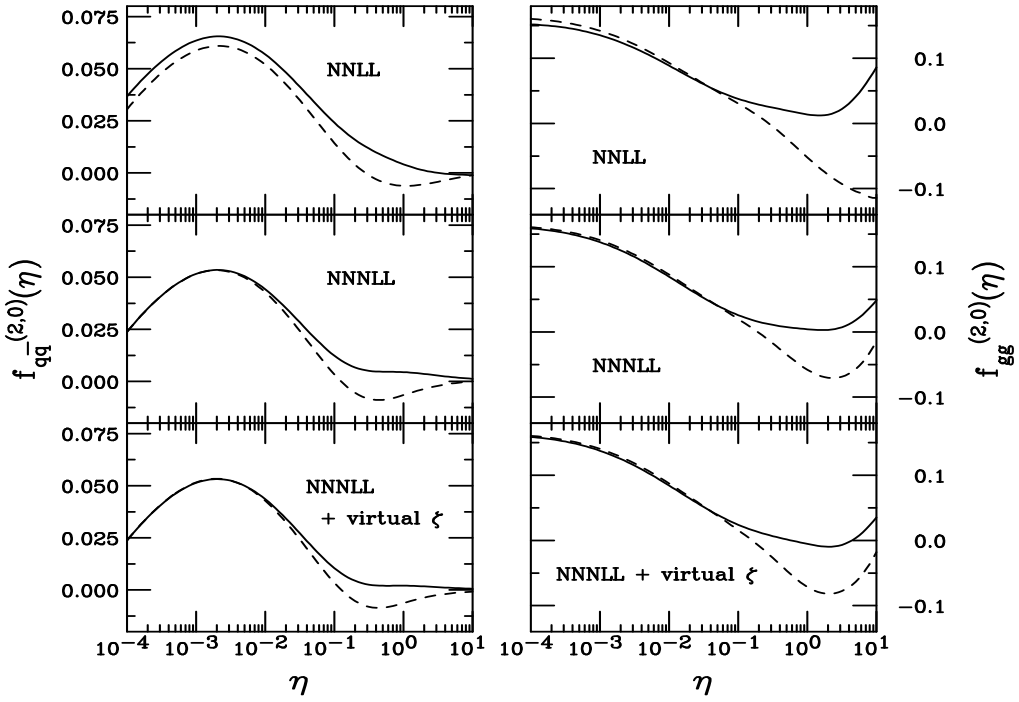

Figure 12: The $f_{ij}^{(2,0)}$ scaling functions in the $\overline{\rm MS}$ scheme. The left-hand side shows the results for the $q\bar{q}$ channel while the right-hand side shows the results for the gg channel. The top plots show the NNLL result. The center plots give the results through NNNLL and the bottom plots give the results including the virtual ζ terms. The solid curves are for 1PI kinematics, the dashed for PIM kinematics. [From Kidonakis and R.V., Phys. Rev. **D 68** (2003) 114014.]

NNLO-NNNLL+ζ $c\bar{c}$ Results

We use MRST2002 NNLO parton densities, unavailable before, with 3-loop evaluation of α_s, as well as GRV98 HO

Compare NLO, NNLO-NNLL and NNLO-NNNLL+ζ 1PI cross sections

Complex color structure of *gg* channel favors 1PI, large negative contribution in PIM kinematics, we only show 1PI results

Study results as a function of m, μ and parton densities

NNLO-NNNLL+ζ $c\bar{c}$ Total Cross Sections: GRV98 HO PDFs

Subleading terms reduce the NNLO-NNNLL+ζ 1PI results relative to NNLO-NNLL, closer to NNLO-NNLL 1PI and PIM average

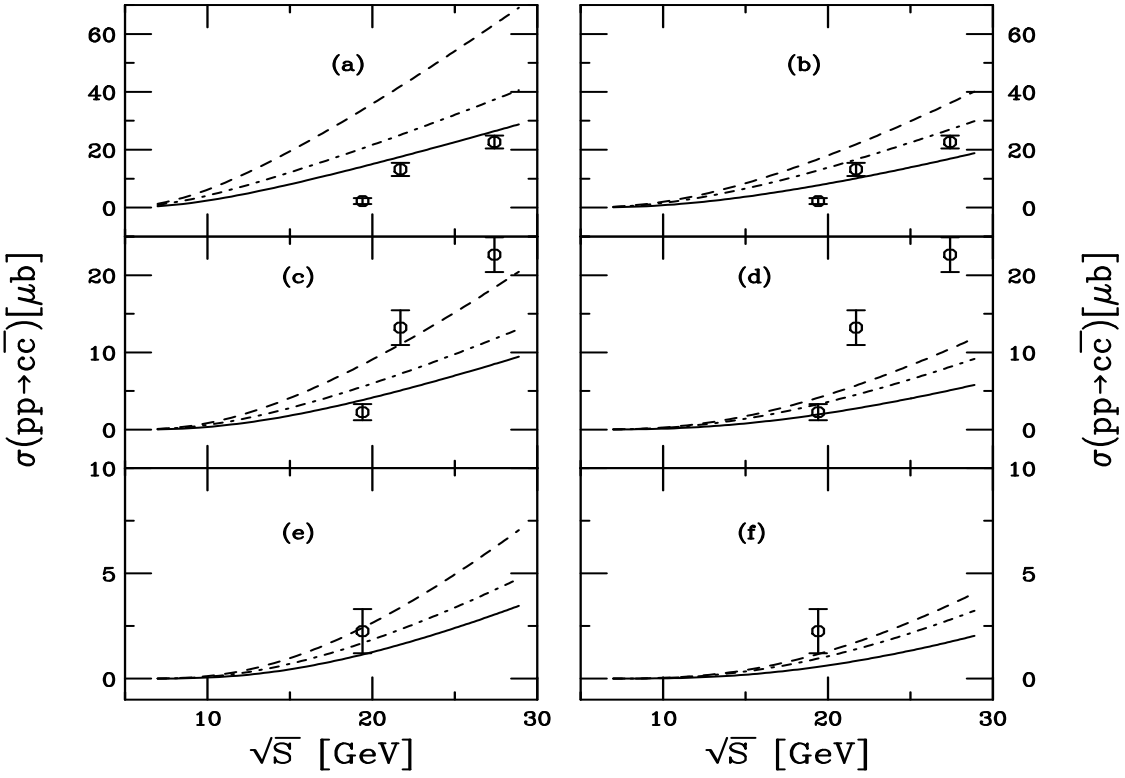

Figure 13: The total $pp \to c\bar{c}$ cross section calculated with the GRV98 HO densities. The upper, middle and lower plots show $m = 1.2$, 1.5 and 1.8 GeV respectively. The left-hand side gives the results for $\mu = m$ while the right-hand side shows the results with $\mu = 2m$. The curves are the NLO (solid), NNLO-NNLL (dot-dashed) and NNLO-NNNLL+ζ (dashed) 1PI results.

NNLO-NNNLL+ζ $c\bar{c}$ Total Cross Sections: MRST2002 NNLO PDFs

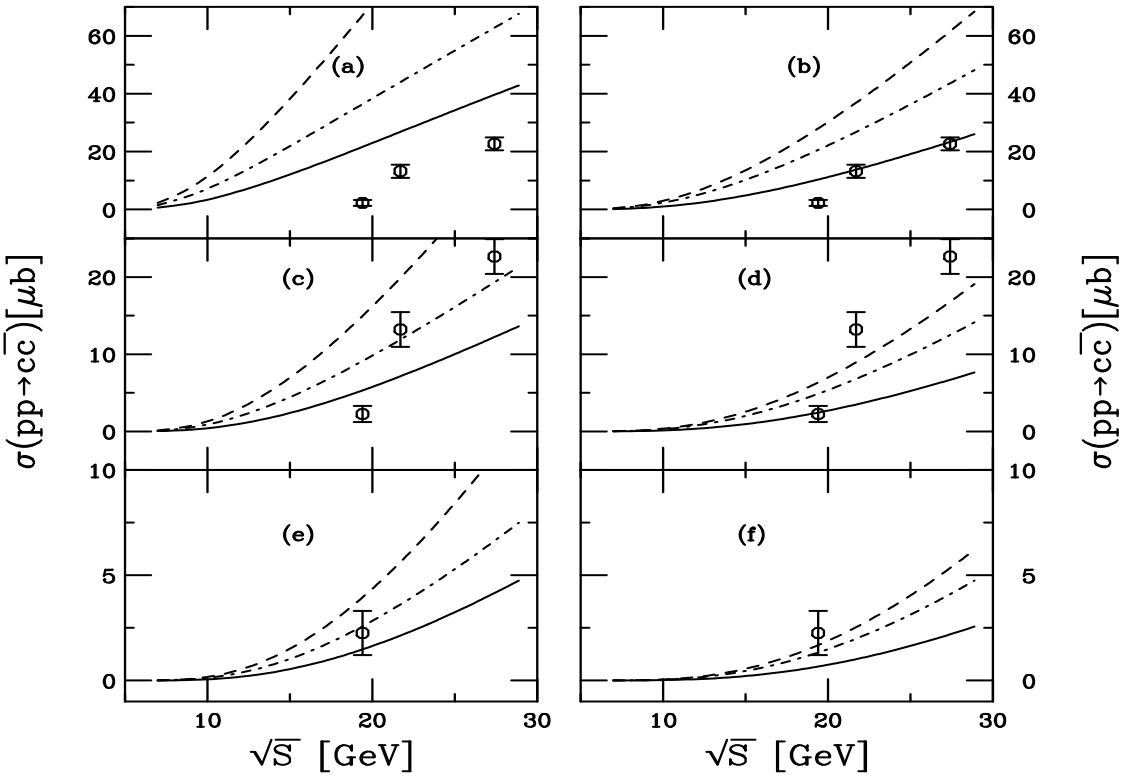

Figure 14: The total $pp \to c\bar{c}$ cross section calculated with the GRV98 HO densities. The upper, middle and lower plots show $m = 1.2$, 1.5 and 1.8 GeV respectively. The left-hand side gives the results for $\mu = m$ while the right-hand side shows the results with $\mu = 2m$. The curves are the NLO (solid), NNLO-NNLL (dot-dashed) and NNLO-NNNLL+ζ (dashed) 1PI results.

NNLO-NNNLL+ζ $c\bar{c}$ K Factors: GRV98 HO PDFs

Subleading terms reduced the NNLO K factor relative to NNLL terms alone

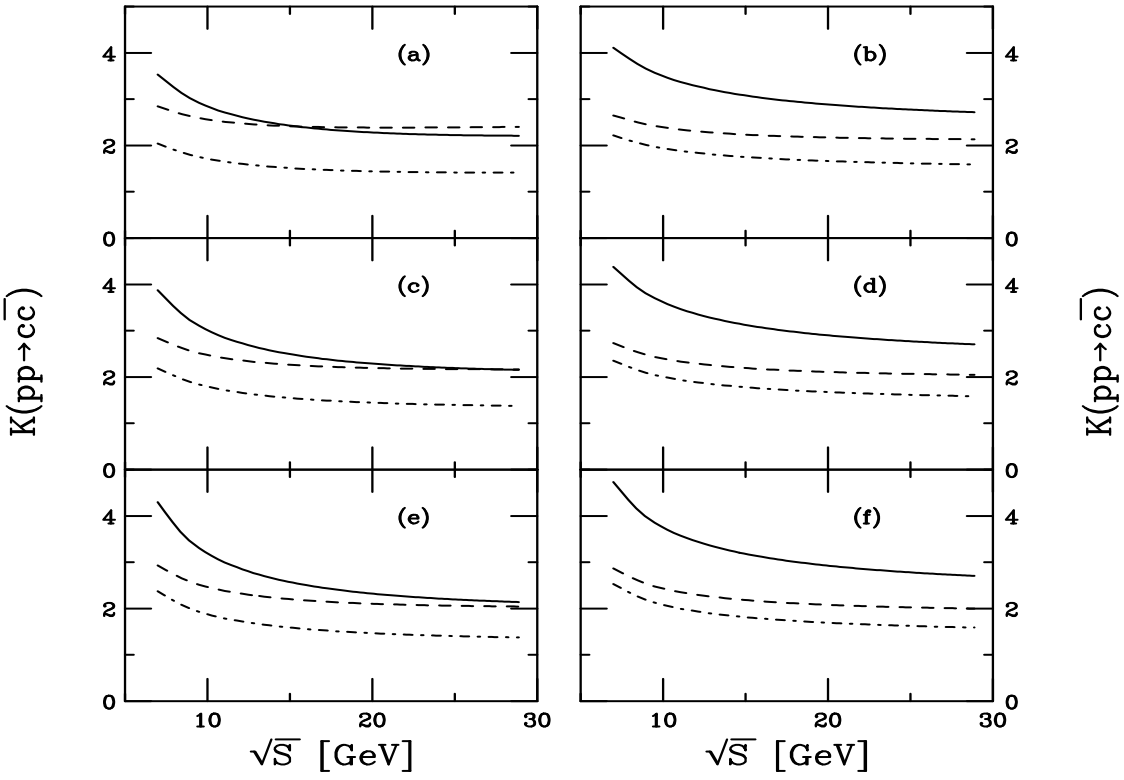

Figure 15: The $c\bar{c}$ K factors calculated with the GRV98 HO densities. The upper, middle and lower plots show $m = 1.2$, 1.5 and 1.8 GeV respectively. The left-hand side gives the results for $\mu = m$ while the right-hand side shows the results with $\mu = 2m$. We give $K_2^{(1)}$ (solid), $K_{1\mathrm{PI}}^{(2)}$ to NNLL (dashed) and $K_{1\mathrm{PI}}^{(2)}$ (dot-dashed) to NNNLL+ζ.

NNLO-NNNLL+ζ $c\bar{c}$ K Factors: MRST2002 NNLO PDFs

K factors larger than for GRV98 HO

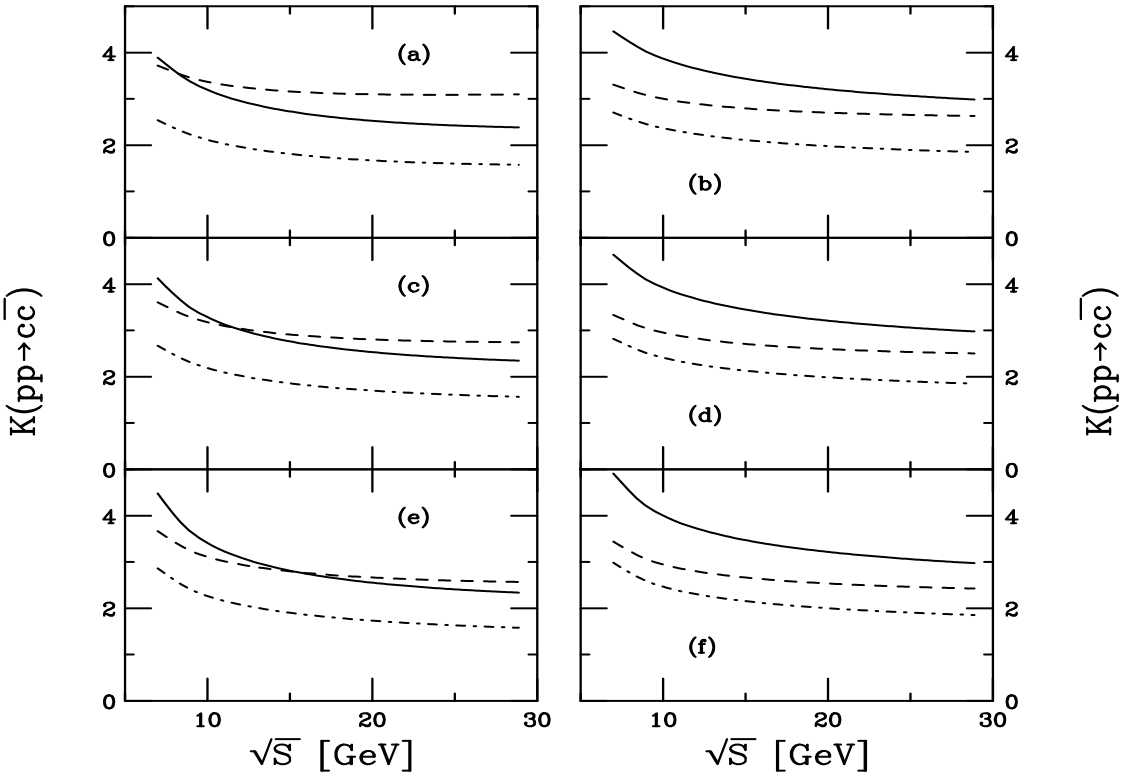

Figure 16: The $c\bar{c}$ K factors calculated with the MRST2002 NNLO densities. The upper, middle and lower plots show $m = 1.2$, 1.5 and 1.8 GeV respectively. The left-hand side gives the results for $\mu = m$ while the right-hand side shows the results with $\mu = 2m$. We give $K_2^{(1)}$ (solid), $K_{1\mathrm{PI}}^{(2)}$ to NNLL (dashed) and $K_{1\mathrm{PI}}^{(2)}$ (dot-dashed) to NNNLL+ζ.

NNLO-NNNLL+ζ $c\bar{c}$ Scale Dependence

Subleading contributions reduce scale dependence beyond NNLO-NNLL

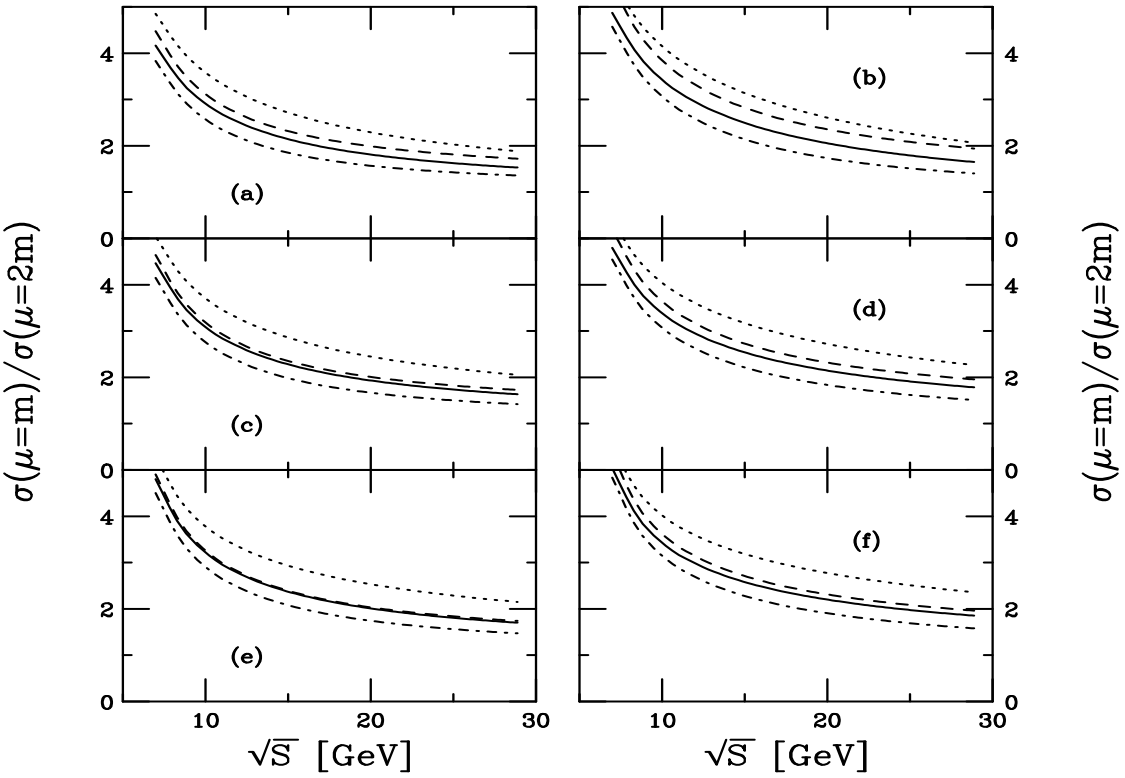

Figure 17: The $c\bar{c}$ scale dependence. The upper, middle and lower plots show $m = 1.2$, 1.5 and 1.8 GeV respectively. The left-hand side gives the results for the GRV98 HO densities while the right-hand side shows the results with MRST2002 NNLO. The LO (dotted), NLO (solid), NNLO-NNLL 1PI (dashed) and NNLO-NNNLL+ζ 1PI (dot-dashed) ratios are shown.

Predicted Charm Cross Sections at GSI and SPS

σ (μb)			
$\sqrt{S}$ (GeV)	Order	MRST2002 NNLO	GRV98
6.98	NLO	$0.034\ ^{+0.56}_{-0.027}\ ^{+0.56}_{-0.032}$	$0.028\ ^{+0.42}_{-0.022}\ ^{+0.42}_{-0.026}$
6.98	NNLO-NNNLL+ζ	$0.09\ ^{+1.4}_{-0.07}\ ^{+1.4}_{-0.085}$	$0.061\ ^{+0.9}_{-0.05}\ ^{+0.9}_{-0.057}$
17.3	NLO	$3.8\ ^{+13}_{-2.1}\ ^{+13}_{-2.8}$	$2.8\ ^{+8.3}_{-1.4}\ ^{+8.3}_{-2}$
17.3	NNLO-NNNLL+ζ	$6.7\ ^{+22.5}_{-3.4}\ ^{+22.5}_{-4.9}$	$4.1\ ^{+12.2}_{-1.8}\ ^{+12.2}_{-3}$

Table 1: The $c\bar{c}$ production cross sections in pp collisions at $\sqrt{S} = 6.98$ and 17.3 GeV. The exact NLO results and the approximate NNLO-NNNLL+ζ results, based on $m = \mu = 1.5$ GeV, are shown. The first uncertainty is due to the scale choice, the second, the charm quark mass.

Summary

- Progress has been made on NNLO heavy quark hadroproduction near threshold
- Complete calculation still unavailable
- Enhancement of charm cross section over NLO is large at GSI